Journal of ELECTRONIC MATERIALS, Vol. 46, No. 10, 2017
DOI: 10.1007/s11664-017-5655-x

Effect of Sn-Ag-Cu on the Improvement of Electromigration Behavior in Sn-58Bi Solder Joint

FENGJIANG WANG,[1,4] LILI ZHOU,[1] ZHIJIE ZHANG,[1] JIHENG WANG,[2,3] XIAOJING WANG,[1] and MINGFANG WU[1]

1.—Provincial Key Lab of Advanced Welding Technology, Jiangsu University of Science and Technology, Zhenjiang 212003, China. 2.—School of Materials Science and Engineering, Jiangsu University of Science and Technology, Zhenjiang 212003, China. 3.—National Demonstration Center for Experimental Materials Science and Engineering Education, Jiangsu University of Science and Technology, Zhenjiang 212003, China. 4.—e-mail: fjwang@just.edu.cn

Reliability issues caused by the formation of a Bi-rich layer at the anode interface usually occurs in the Sn-58Bi eutectic solder joint during electromigration (EM). To improve the EM performance of a Sn-58Bi solder joint, Sn-3.0Ag-0.5Cu solder was introduced into it to produce SnBi-SnAgCu structural or compositional composite joints, and their EM behaviors were investigated with the current density of 1.0×10^4 A/cm^2 for different stressing times. The structure of the compositional composite solder joint was obtained by the occurrence of partial or full mixing between Sn-Bi and Sn-Ag-Cu solder with a suitable soldering temperature. In the structural composite joint, melted Sn-Bi was partially mixed with Sn-Ag-Cu solder to produce a Cu/Sn-Bi/Sn-Ag-Cu/Sn-Bi/Cu structure. In the compositional composite joint, full melting and mixing between these two solders occurred to produce a Cu/Sn-Ag-Cu-Bi/Cu structure, in which the solder matrix was a homogeneous structure including Sn, Bi phases, Cu_6Sn_5 and Ag_3Sn IMCs. After current stressing, the EM performance of Sn-Bi solder was obviously improved with the structural or the compositional composite joint. In Sn-58Bi joints, a thick Bi-rich layer was easily produced at the anode interface, and obviously increased with stressing time. However, after current stressing on the structural composite joints, the existence of s Sn-3.0Ag-0.5Cu interlayer between the two Sn-58Bi solders effectively acted as a diffusion barrier and significantly slowed the formation of the Bi-rich layer at the anode side and the IMC thicknesses at the interfaces.

Key words: Electromigration, Sn-Bi, Sn-Ag-Cu, composite joint, Bi segregation

INTRODUCTION

Electromigration (EM) has become an important reliability issue with the miniaturization of electronic products and increasing electric current density in microelectronic devices. EM is generally considered to be the result of atomic directional diffusion driven by the electron wind force,[1] and the phenomenon of phase separation is likely to occur under EM due to the different atomic diffusivities in the solder joints, which has been widely reported in the commonly used binary solder alloys, such as Pb precipitation at the anode in Sn-37Pb,[2] migration of Zn towards the cathode in Sn-9Zn,[3–5] and In segregation at the cathode in Sn-52In.[6,7] Phase segregation and the resulting polarity effect or the reverse polarity effect on intermetallic compound (IMC) growth at the interface then result in the earlier failure from voids nucleation and propagation in the solder joints.[8]

(Received September 25, 2016; accepted June 15, 2017; published online June 26, 2017)

Sn-58Bi eutectic solder is a preferable solder for low-temperature applications, due to its low melting point (138°C) and coefficient of thermal expansion. Under current stressing in EM, Bi atoms also migrate along the direction of electron flowing and produce Bi segregation at the anode.[9–11] Many efforts have been made to inhibit the EM phenomenon in Sn-Bi solder joints, such as applying the plastic pre-straining on the solder interconnects,[12] but alloying Sn-Bi solder with a third component was the most commonly used method. The verified effective elements include Ag,[13,14] Ag nanoparticles,[15] Ni particles,[16] rare earth,[17] nano-Al_2O_3 particles,[18] graphene nanosheets,[19] etc.

In this paper, we selected Sn-3.0Ag-0.5Cu Pb-free solder as the diffusion barrier to improve the EM performance of Sn-58Bi solder. Sn-Ag-Cu is the most common used Pb-free solder alloy, and has a melting point of 217–221°C.[20] Assembling Sn-Ag-Cu ball with Sn-Bi paste also provides a lower-temperature soldering process. Due to the difference in the melting point of Sn-Ag-Cu and Sn-Bi, partial mixing or full mixing between them will occur with the peak reflowing temperature below 217°C or above 221°C, respectively, and then produce a structural or a compositional composite solder joint. Therefore, a simplified line-type Cu/Sn-58Bi/Sn-3.0Ag-0.5Cu/Sn-58Bi/Cu solder joint was designed to investigate the effect of Sn-3.0Ag-0.5Cu interlayer on the interfacial evolution between Sn-Bi and Cu. Also, partial or full mixing between Sn-Bi and Sn-Ag-Cu in the joints was considered during EM.

EXPERIMENTAL

The solder alloys used in this paper are Sn-58Bi and Sn-3.0Ag-0.5Cu preforms supplied by Guangzhou XianYi Electronic Technology, with the thickness of 100 μm, 200 μm, and 300 μm, respectively. The Cu substrate was from commercial purity (99.9 wt.%) oxygen-free Cu in a dimension of 15 mm × 15 mm × 0.5 mm. The line-type joints were fabricated with the methods shown in Fig. 1 and the details illustrated in our previous work.[21,22] The Cu plates were metallographically polished and ultrasonic cleaned with acetone and distilled water before soldering. The reflowing temperature was carefully selected according to the melting point of Sn-58Bi and Sn-3.0Ag-0.5Cu. In the Cu/Sn-Bi/Cu uniform joint, a Sn-58Bi solder with the thickness of 300 μm was used, and the peak soldering temperature was 175°C. In Cu/Sn-Bi/Sn-Ag-Cu/Sn-Bi/Cu mixed joints, the thicknesses of Sn-Bi and Sn-Ag-Cu Pb-free were 100 μm and 200 μm, respectively. To obtain the structural composite solder joint with partial mixing between Sn-Bi and Sn-Ag-Cu, the reflowing temperature was selected as 175°C. Melted Sn-Bi solder was capable of wetting the Cu substrate and partially dissolved by solid Sn-Ag-Cu solder. To obtain the compositional solder joint with full mixing between Sn-Bi and Sn-Ag-Cu, the peak temperature during reflow soldering was set at 260°C to guarantee the adequate melting and mixing between solders. The soldering time was 30 s for all joints. After soldering, the joints were cut and polished to a thin bar with a cross-section of 0.3 mm × 0.3 mm and a length of 30 mm.

The electromigration test on each sample was performed with a calculated current density of 1.0×10^4 A/cm^2 and EM time ranged from 0 to 264 h. Since the Joule heating will generate most of the heat in the solder joints, the samples were immersed into the silicone oil during EM. To monitor the temperature increase on the solder joint caused by EM, a thermocouple was placed beside the solder joint, and the result showed that the temperature around the sample first increased rapidly and then reached a stable value of 55 ± 5°C after about 10 min. After EM, a common metallographic preparation method was used for all samples. The interfacial microstructure in the solder joints was observed by scanning electron microscopy (SEM), and the phase compositions were detected by energy dispersive x-ray spectroscopy (EDS).

RESULTS AND DISCUSSION

As-Soldered Joints

Figure 2 shows the back-scattered electronic (BSE) images on the cross-sectional microstructure of the whole solder joint, the interfacial microstructure at solder/Cu, and the microstructure in the solder matrix for Sn-58Bi (Fig. 2a–c), structural composite (Fig. 2d–f) and compositional composite solder joints (Fig. 2g–i), respectively. It can be found that the line-type solder joints without the obvious voids were successfully achieved with the method given in Fig. 1. In the Sn-58Bi solder joint, the solder was melted and wetted with the Cu substrate to form a very thin IMC layer at the solder/Cu interface, as shown in Fig. 2b. The solder matrix in Fig. 2c for the Sn-58Bi solder was uniformly composed of the gray Sn-rich phases and the white Bi-rich phases, a typical eutectic two-phase microstructure. In the SnBi-SnAgCu structural composite solder joint, because the selected soldering temperature at 175°C was lower than the melting point of Sn-3.0Ag-0.5Cu solder (217–221°C), the Sn-Ag-Cu solder was kept as the solid interlayer, while melted Sn-58Bi solder was wetted with both Cu and Sn-3.0Ag-0.5Cu solder to produce a structural composite solder joint, as shown in Fig. 2d. At the interface between the Sn-58Bi solder and Cu in Fig. 2e, a thin IMC layer was also formed due to the reaction between them. At the interface between Sn-58Bi and Sn-3.0Ag-0.5Cu solders given in Fig. 2f, a boundary was easily observed between them, but the metallurgical bonding was capable of being achieved due to the mutual solid solution in these two solders. In the SnBi-SnAgCu compositional composite solder joint, the soldering temperature was selected as 260°C. Therefore, full mixing

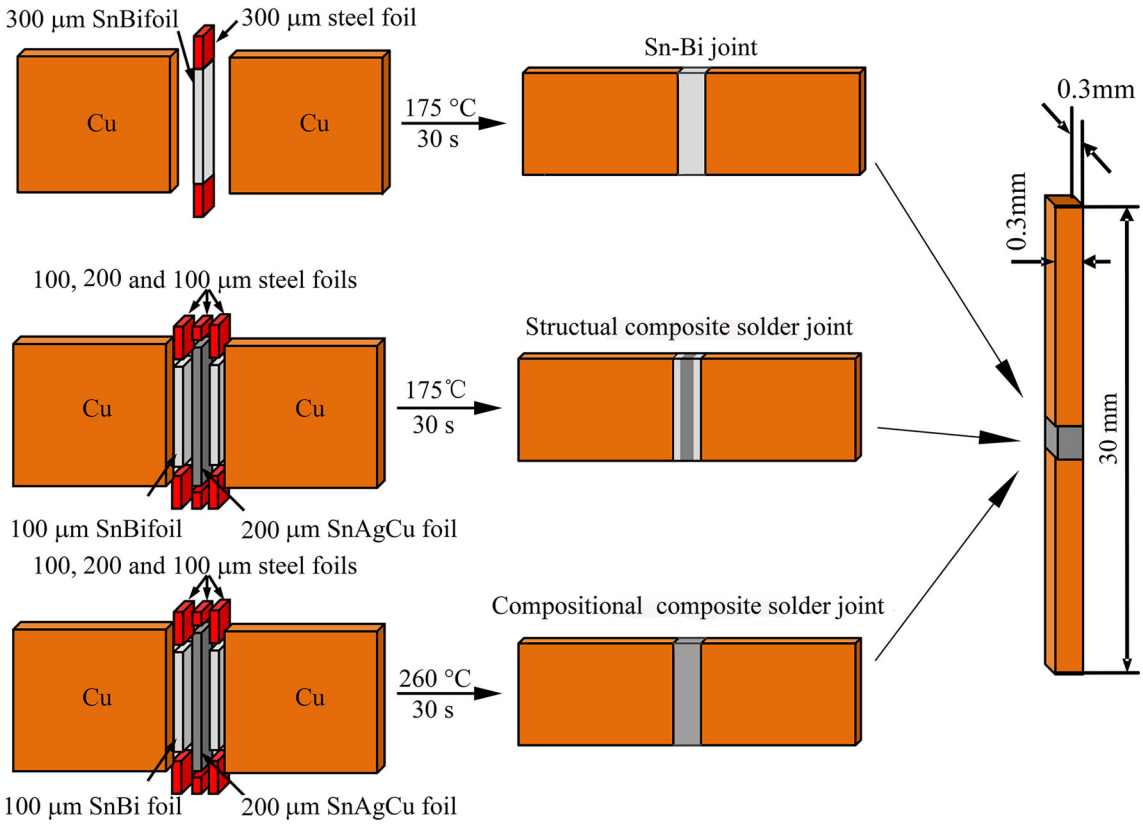

Fig. 1. Schematic on preparation of line-type Cu/solder/Cu joints.

occurred between the melted Sn-58Bi and Sn-3.0Ag-0.5Cu solders to produce a homogeneous Sn-Ag-Cu-Bi structure, in which Cu_6Sn_5, Ag_3Sn and Bi phases were uniformly distributed in the Sn-based solder matrix, as seen in Fig. 2i. An IMC layer was also observed at the interface of the solder/Cu in Fig. 2h, but was relatively thicker than those observed in Fig. 2b and e due to the higher soldering temperature. The composition of these IMCs was confirmed as Cu_6Sn_5 phase according to the EDS results.

Effect of Current Stressing on Cu/Sn-58Bi/Cu Joints

Figure 3 shows the BSE images on the microstructural evolution of the anode and cathode interface of the Cu/Sn-58Bi/Cu joint with the increasing stressing times under the current density of 1.0×10^4 A/cm^2 at room temperature, in which the arrow with symbol 'e-' illustrates the direction of electron flow. The images on the left-hand and right-hand side columns represent the interfacial structures at the anode and cathode sides, respectively.

At the anode side, Fig. 3a displays the interfacial microstructure of the Sn-58Bi solder joint after current stressing for 33 h. Compared with the as-soldered microstructure without current stressing, both the Sn-rich phase and the Bi-rich phase were obviously coarsened in the solder matrix. The most interesting phenomenon was that a white Bi-rich layer accumulated at the interface between the IMC layer and solder, and its average thickness was about 6 μm. The thickness of the Cu-Sn IMC layer increased, and the morphology of IMC was also flattened. With the current stressing time increasing, there were small changes in the thickness and shape of the IMCs, but the thickness of the Bi-rich layers had an obvious tendency to increase with time, as observed in Fig. 3c for 99 h and Fig. 3e for 132 h. This agreed well with the findings of Gu et al. that a Bi-rich layer formed at the anode side in the eutectic Sn-Bi solder during the EM test.[10,11] However, it should be mentioned that the growth rate of IMC layer was very slow because the segregated Bi-rich layer acted as a diffusion barrier at the anode side to prohibit the diffusion reaction between the Sn atoms and the Cu atoms.

At the cathode side, it is clearly seen in Fig. 3 that the microstructure is very different from that at the anode sides. Figure 3b shows the cathodic reaction under 1.0×10^4 A/cm^2 for 33 h. Due to the migration of Bi from the cathode to the anode, there was a gray Sn-rich layer left beside the IMC layer at the cathode side. With the current stressing time increasing, the thickness of the IMC layers grew slowly, but the IMC layer was always thicker than that at the anode side with the same stressing time. In other words, the growth rate of the IMC layer at

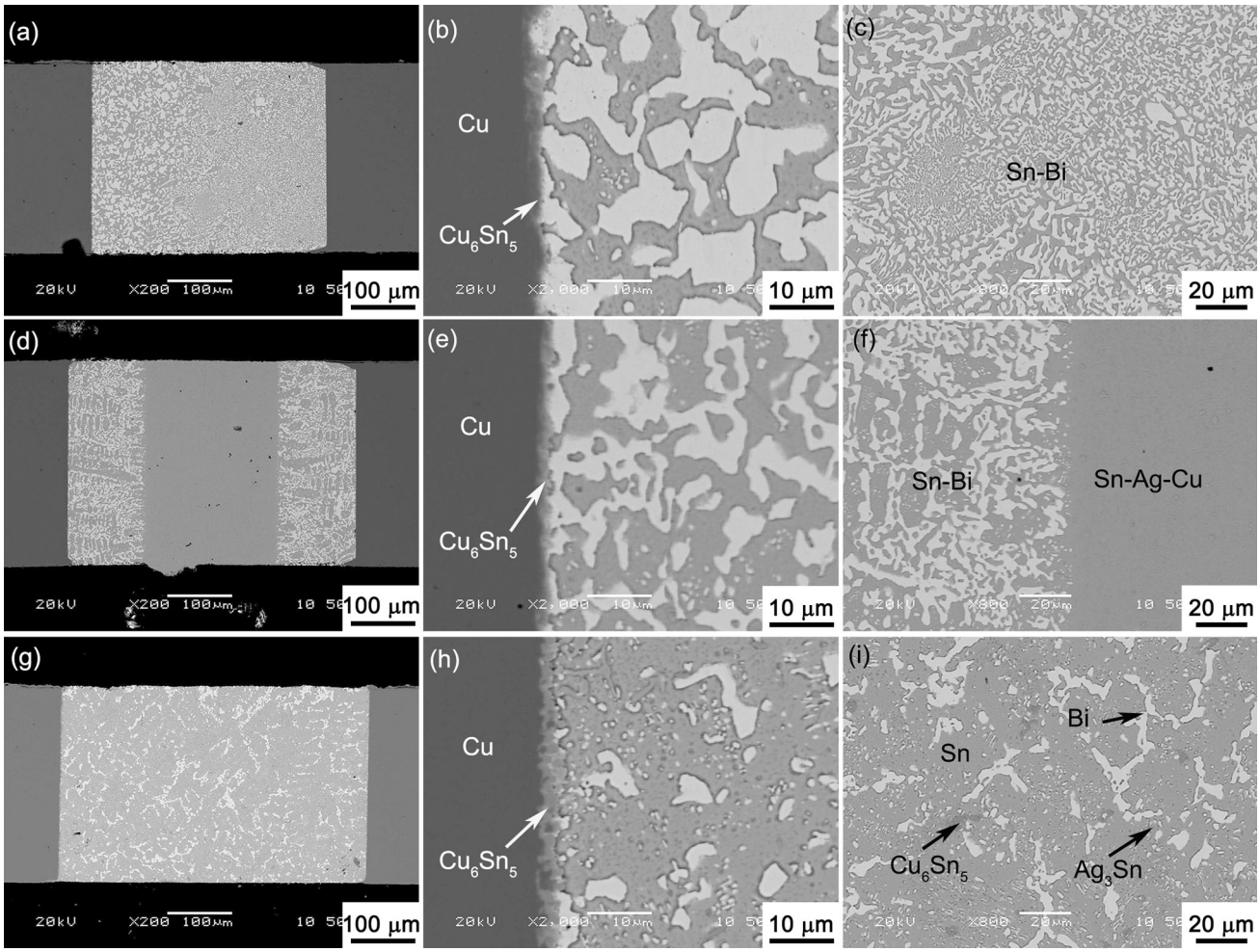

Fig. 2. Backscattered electron (BSE) images of the cross-sectional microstructure of (a)–(c) Sn-58Bi, (d)–(f) SnBi-SnAgCu structural composite and (g)–(i) SnBi-SnAgCu compositional composite solder joints: (a), (d) and (g) represent the whole solder joint, (b), (e) and (h) represent the interfacial microstructure between solder and Cu, and (c), (f) and (i) represent the microstructure in the solder matrix.

the anode side was slower than that of the cathode during EM because the Cu atoms were driven by the electron flow and migrated toward the anode side. Furthermore, the Sn-rich phase and its thickness increased with the stressing time. A Sn-rich layer was clearly observed under a prolonged stressing time for 132 h, as shown in Fig. 3f. However, comparing the cathode with the anode interface, the thickness of the Sn-rich layers was always thinner than that of the Bi-rich layers under the same stressing time.

Effect of Current Stressing on Composite Solder Joints

Figure 4 shows the interfacial images of the line-type Cu/Sn-58Bi/Sn-3.0Ag-0.5Cu/Sn-58Bi/Cu structural composite solder joints at the current density of 1.0×10^4 A/cm^2 for 33 h, 66 h, 99 h, and 132 h, respectively. In the structural composite solder joints, the microstructure in the solder matrix is still a typical two-phase structure with white Bi phases and gray Sn phases after current stressing. It can also be found that these phases were coarsened with the stressing time. At the anode side with the stressing time reaching 33 h, as shown in Fig. 4a, no obvious Bi-rich layer was formed at the interface. After 66 h, as shown in Fig. 4c, the thickness of the IMC layer increased and a thin Bi layer began to form between the solder and the Cu substrate with the arrival of Cu, Sn and Bi atoms to the anode interface, and the thickness of the Bi-rich layer was about 4 μm. With the stressing time increasing, the thickness of the IMC increased slowly but the continuous migration of Bi atoms promoted their accumulation at the anode side. Compared with the anode sides in the Sn-58Bi solder joints, after the same current stressing time for 132 h, the thickness of the white Bi layer was about 7 μm in the structural composite solder joint (Fig. 4g), while it was about 22 μm in the Sn-58Bi solder joint (Fig. 3e). Figure 4b, d, f, and h shows the interfaces at the cathode side in the structural composite solder joints with different stressing

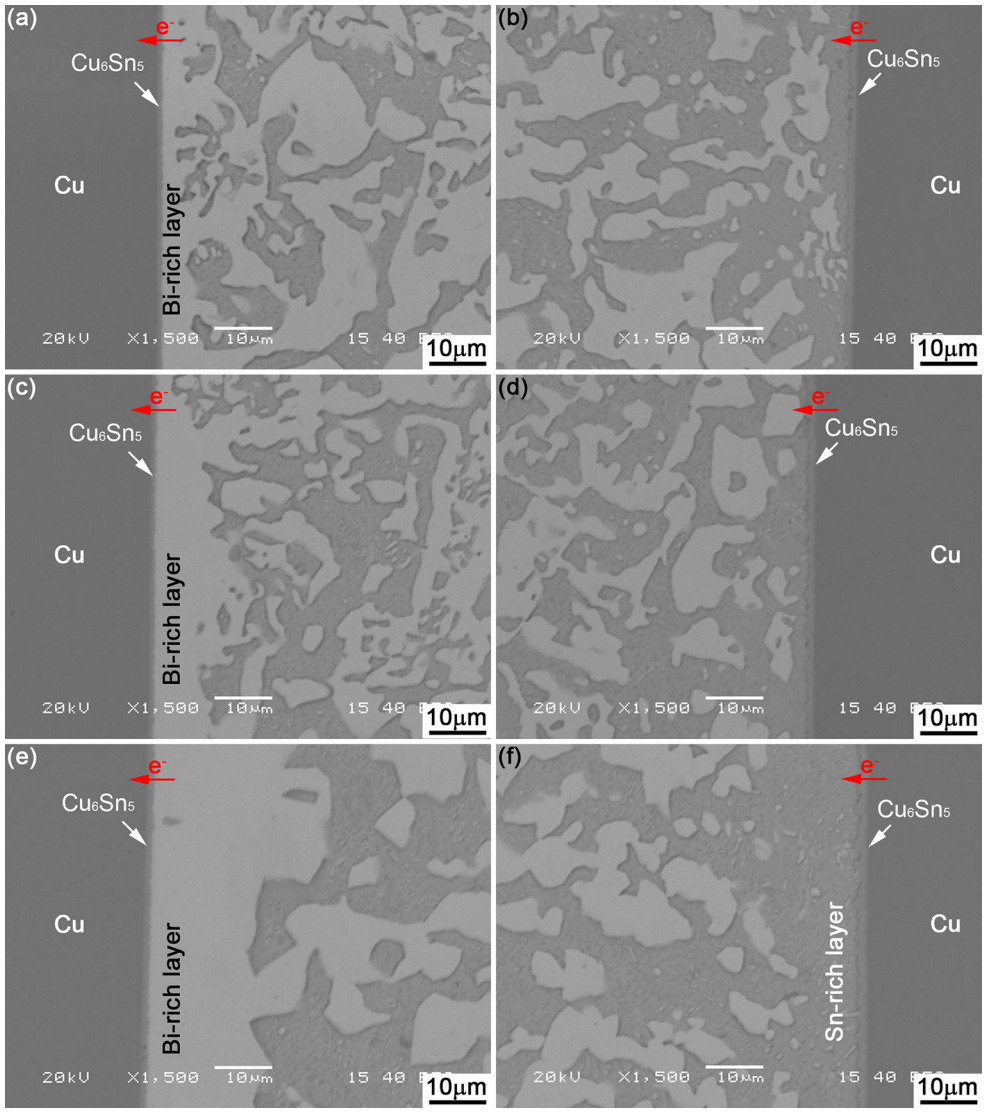

Fig. 3. BSE images on the interfacial structures in the line-type Cu/Sn-58Bi/Cu solder joints after current stressing of 1.0×10^4 A/cm^2 for (a) 33 h at the anode side, (b) 33 h at the cathode side, (c) 99 h at the anode side, (d) 99 h at the cathode side, (e) 132 h at the anode side, and (f) 132 h at the cathode side.

times. Under the electron flow, the Bi atoms were increasingly expelled from the cathode, but there was no obvious Sn-rich layer observed at the interface. It seems that the Sn-3.0Ag-0.5Cu interlayer in the structural composite solder joints hampered the migration of not only the Bi atoms but also the Sn atoms, and then depressed the segregation of the Sn and Bi atoms in the Sn-Bi solder.

Figure 5 shows the interfacial images of the line-type Cu/Sn-58Bi/Sn-3.0Ag-0.5Cu/Sn-58Bi/Cu compositional composite solder joints after current stressing for 33 h, 99 h, 132 h, and 264 h, respectively. In the compositional composite solder joint, its composition was close to the Sn-1.5Ag-0.5Cu-29Bi solder due to the full melting and mixing between the Sn-58Bi and Sn-3.0Ag-0.5Cu solders with the ratio about 1:1. It was mentioned that the structure in the solder matrix was mainly composed of Sn-rich phases, Bi-rich phases, Cu_6Sn_5 and Ag_3Sn IMCs. Therefore, the microstructure in the solder matrix shown in Fig. 5 was completely different from that observed in the Sn-58Bi joints (as seen in Fig. 3) or in the structural composite joints (as seen in Fig. 4). At the anode side in the compositional solder joints, the segregation of Bi-rich layers completely disappeared in Fig. 5a and c with the current stressing time of 33 h and 99 h. With a prolonged stressing time of 132 h, a non-continuous thin Bi layer began to be observed in Fig. 5e. To study the Bi segregation at the anode side in the compositional joint, the joint was further current-stressed to a prolonged time of 264 h, as shown in Fig. 5g, and then an obvious Bi-rich layer was observed at the interface with the thickness of only about 6 μm. Figure 5b, d, f, and h shows the

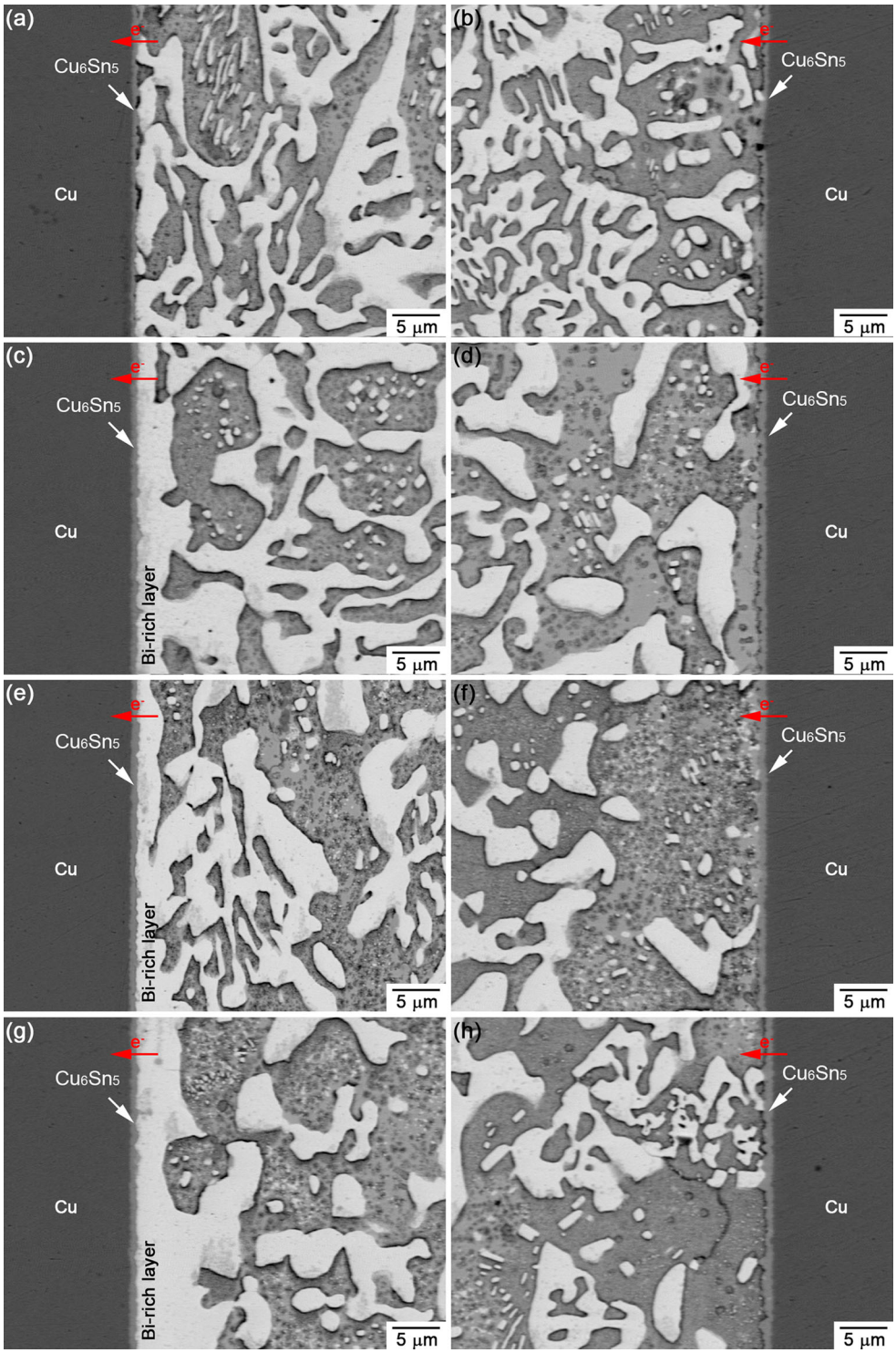

Fig. 4. BSE images on the interfacial structures in the line-type structural composite solder joints after current stressing of 1.0×10^4 A/cm^2 for (a) 33 h at the anode side, (b) 33 h at the cathode side, (c) 66 h at the anode side, (d) 66 h at the cathode side, (e) 99 h at the anode side, (f) 99 h at the cathode side, (g) 132 h at the anode side, and (h) 132 h at the cathode side.

interfaces at the cathode sides of the compositional composite solder joints under the current density 1.0×10^4 A/cm^2 for 33 h, 99 h, 132 h, and 264 h, respectively. There were no obvious changes on the shape and thickness of the IMC, and also the solder matrix was similar to the anode microstructure under the same stressing time. However, it can be observed from Fig. 5 that more scallop-type IMCs were produced at the anode and cathode interfaces in the compositional joints compared with the

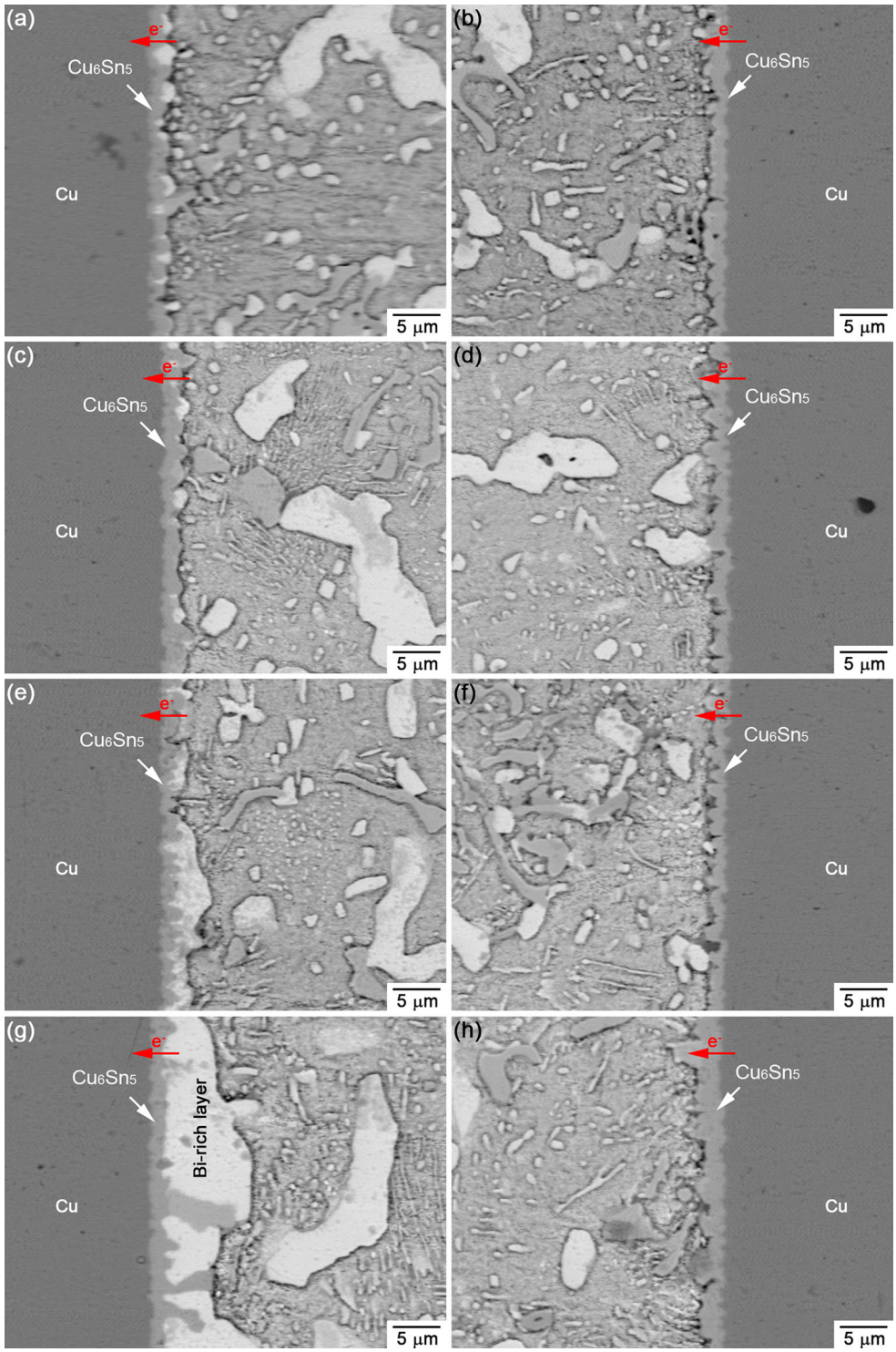

Fig. 5. BSE images on the interfacial structures in the line-type compositional composite solder joints after current stressing of 1.0×10^4 A/cm^2 for (a) 33 h at the anode side, (b) 33 h at the cathode side, (c) 99 h at the anode side, (d) 99 h at the cathode side, (e) 132 h at the anode side, (f) 132 h at the cathode side, (g) 264 h at the anode side, and (h) 264 h at the cathode side.

flattened morphologies in the Sn-58Bi joints and the structural compositional joints, which was attributed to the reason that the formation of Bi-rich layer at the anode prohibited the diffusion of Cu and Sn atoms and the reaction between them.

The thickness of the Bi-rich layers at the anode sides was measured from the SEM images and was then plotted in Fig. 6 with the effect of current stressing periods and joint configuration. It should be noted that the maximum current stressing time

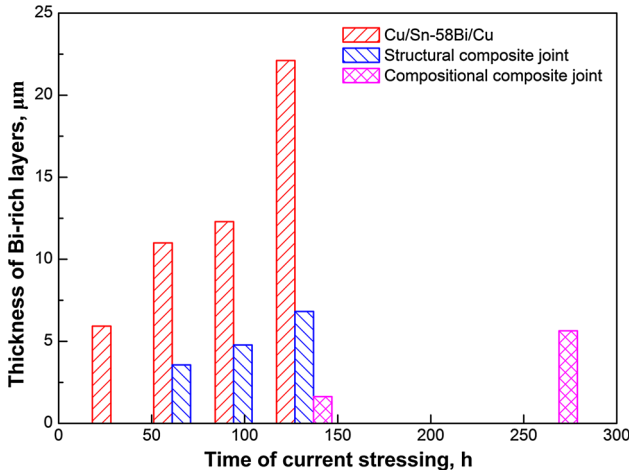

Fig. 6. Changes in the thickness of the Bi-rich layer at the anode interfaces with stressing time.

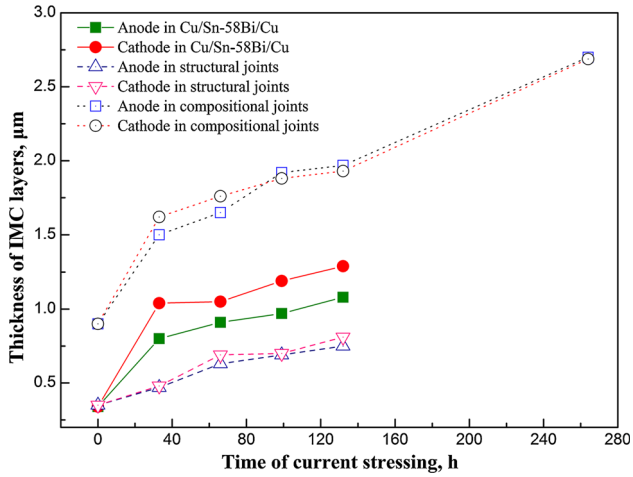

Fig. 7. Changes in the thickness of the Cu-Sn IMCs layer with current stressing time.

was 132 h for the Sn-58Bi and structural composite joints and 264 h for the compositional composite joints, respectively. As seen in Fig. 6, a thick Bi-rich layer was easily produced in the Sn-58Bi joints. The thickness of the Bi-rich layer increased quickly with increasing the current stressing time, and reached to about 22 μm after 132 h. In the structural composite solder joints, the thickness of the Bi-rich layer at the interface was obviously depressed. Therefore, the un-melted Sn-3.0Ag-0.5Cu interlayer in the structural composite joint played a retardant role on the migration of Bi phases from the Sn-Bi solder. After the joint configuration was transformed from structural composite to compositional composite, the formation of the Bi-rich layer at the anode side was further depressed. It was only produced after a longer current stressing time, and its thickness was about 6 μm even after 264 h. Therefore, it seems that the dissolution of Sn-Ag-Cu solder into Sn-Bi solder played a more effective role on the depressing effect of formation of the Bi-rich layer. After the Sn-3.0Ag-0.5Cu solder was dissolved into the Sn-58Bi solder, the amount of the Bi phases decreased, while the Ag_3Sn and Cu_6Sn_5 IMCs were uniformly distributed in the solder matrix. In fact, Sun et al.[14,15] have reported that a small addition of Ag into Sn-58Bi solder was beneficial in decreasing the formation of the Bi-rich layer. On the other hand, Tian[21] studied the EM behavior of Cu/Sn-Pb/Sn-Ag-Cu/Cu structural joints and found that the Ag_3Sn network in Sn-Ag-Cu solder prohibited the migration of Sn and Pb atoms. Therefore, it seems that the uniform distribution of IMCs in the solder matrix also prohibited the migration of Sn and Bi atoms during EM.

On the other hand, the thicknesses of the Cu-Sn IMCs layers were also measured, with the results plotted in Fig. 7. In the Sn-58Bi solder joints, the thickness of the IMC layer at the anode and cathode sides increased with the current stressing time, but the growth rate obviously decreased after 33 h due to the diffusion barrier from the existence of the Bi-rich layer at the anode interface. Also, the thickness of the IMC at the cathode interface always grew faster than that at the anode side due to the migration of Sn atoms from the anode to the cathode. Comparing the structural joints with the Sn-58Bi joints, the growth rate of the IMC layer at the interface was a little slower. This phenomenon can also be possibly attributed to the formation of the Bi-rich layer at the anode interface and the existence of a solid Sn-3.0Ag-0.5Cu interlayer. The decrease of the Bi-rich layer in the structural joints illustrated that the diffusion of Bi atoms from the cathode to the anode and the Sn atoms from the anode to the cathode under the electron flow were both partially blocked by the Sn-3.0Ag-0.5Cu interlayer. However, comparing the compositional composite solder joints with the Sn-58Bi joints, the thickness of the interfacial IMC layer was greater in the compositional joints due to the higher content of Sn in the solder matrix and the lack of the Bi-rich layer at the interface. Also, the higher soldering temperature produced a thicker initial thickness for the IMC layer for the compositional joint.

During EM, the atomic flux of Bi atoms (J_{EM}) in Sn-Bi joints is composed of the flux from mass accumulation (J_m) and the flux from grain growth (J_g); the flux J_g is one order of magnitude lower than J_m, and can be neglected.[23] Therefore, the atomic flux of Bi atoms can be described with the following equation[23]:

$$J_{EM} = r \times d \times \frac{N}{m} \times 57\% \quad (1)$$

where r is the accumulation rate of Bi, d is the density of Bi (9.8 g/cm^3), N is Avogadro's number (6.02×10^{23} atoms/mol), and m is the atomic weight of Bi (208.98 g/mol). With the accumulation rate of the Bi layer from Fig. 6, the atomic flux of Bi atoms

J_{EM} can be calculated with the results of 5.5×10^{13} atoms/cm^2 s, 2.12×10^{13} atoms/cm^2 s, and 9.29×10^{12} atoms/cm^2 s for Sn-58Bi, the structural composite joint and the compositional composite joint, respectively. Therefore, both the structural composite and the compositional composite with Sn-Ag-Cu in Sn-Bi were beneficial in decreasing the atomic flux of Bi atoms to the anode side.

It should be mentioned that, with a high current density (1.0×10^4 A/cm^2), the local temperature of the solder joint was higher than room temperature due to Joule heating. According to Chen et al.,[24] the heating power (P) can be expressed as:

$$P = I^2R = j^2\rho V \quad (2)$$

where I is the current, R is the resistance, j is the current density, ρ is the resistivity, and V is the volume. The electrical resistivities of Sn-58Bi and eutectic Sn-Ag-Cu are 35 $\mu\Omega$ cm and 15 $\mu\Omega$ cm, respectively. The volumes of the structural composite and compositional composite solder joint are larger than the Cu/Sn-58Bi/Cu solder joint. However, the electrical resistivity of Sn-58Bi is markedly higher than the other two composite solder joints. Thus, the generated Joule heating effect should be the largest in the Sn-58Bi solder joints. For Sn-58Bi, the Joule heating per unit volume per unit time $j^2\rho$ is 3.5×10^2 J/cm^{3}s. The temperature increase from Joule heating will accelerate the atomic activity and the atomic transport. In this study, the simethicone with good thermal conductivity was helpful in decreasing the temperature in the solder joints caused by Joule heating, and the real temperature in the three kinds of solder joints was about 55 ± 5°C. Therefore, the atomic transport caused by Joule heating should be similar, and then was mainly inhibited by the diffusion path in the composite solder joints, which was blocked by the Sn-Ag-Cu interlayer in the structural joints and the IMC particles in the compositional joints.

CONCLUSIONS

To control the formation of the Bi-rich layer in the Sn-58Bi solder joint after EM, a Cu/Sn-58Bi/Sn-3.0Ag-0.5Cu/Sn-58Bi/Cu composite joint was designed to study the effect of composite solder on the EM behavior of Sn-Bi under the current stressing of 1.0×10^4 A/cm^2 at room temperature with different stressing times. The following conclusions can be conidered:

1. Structural composite and compositional composite solder joints were manufactured by controlling partial and full mixing between Sn-58Bi and Sn-3.0Ag-0.5Cu solder with a suitable reflowing temperature. In the structural composite joint, melted Sn-58Bi solder wetted the Cu pad to produce a thin layer of Cu_6Sn_5 IMC, and was partially mixed with Sn-3.0Ag-0.5Cu solder. The joint was composed of a Cu/Sn-Bi/Sn-Ag-Cu/Sn-Bi/Cu structure. In the compositional composite joint, full mixing between the melted Sn-Bi and Sn-Ag-Cu solders occurred to produce a homogeneous structure in the solder matrix composed of Sn phase, Bi phases, Cu_6Sn_5 and Ag_3Sn IMCs, and the joint was composed of a Cu/Sn-Ag-Cu-Bi/Cu structure.
2. After EM on the Sn-58Bi solder joint, a Bi-rich layer was easily formed at the anode side, and quickly increased with current stressing time, while a Sn-rich layer was formed at the cathode side. Meanwhile, the IMC layers at both the anode and the cathode increased after EM, but the growth rate at the cathode side was faster than that at the anode side.
3. After EM on the structural composite joint, the existence of the Sn-3.0Ag-0.5Cu interlayer between the two Sn-58Bi solders effectively acted as a diffusion barrier which blocked the diffusion of Sn and Bi atoms under the electron flow. Therefore, the Bi-rich layer at the anode side and the IMC thicknesses at the interfaces were markedly decreased, although they also increased with stressing time.
4. After EM on the compositional composite joint, the Bi-rich layer at the anode side was almost completely depressed, and can only be observed with a very prolonged stressing time. Correspondingly, the thickness of the IMC at the interface exhibited a slight increase due to the lack of the Bi-rich diffusion barrier and also the higher soldering temperature.

ACKNOWLEDGEMENTS

This research is supported by projects funded by National Natural Science Foundation of China (Grant No. 51541104) and Jiangsu Planning Project of Science and Technology (Grant Nos. BK2012163, BK20150466).

CONFLICT OF INTEREST

The authors declare that they have no conflict of interest.

REFERENCES

1. C. Chen, H.M. Tong, and K.N. Tu, *Annu. Rev. Mater. Res.* 40, 531 (2010).
2. C.-N. Liao, C.-P. Chung, and W.-T. Chen, *J. Mater. Res.* 20, 3425 (2005).
3. M.L. Huang, Z.J. Zhang, N. Zhao, and F. Yang, *J. Alloys Compd.* 619, 667 (2015).
4. M.L. Huang, Q. Zhao, N. Zhao, X.Y. Liu, and Z.J. Zhang, *J. Mater. Sci.* 49, 1755 (2014).
5. X.F. Zhang, J.D. Guo, and J.K. Shang, *J. Mater. Res.* 23, 3370 (2008).
6. Y. Li, A.B.Y. Lim, K.M. Luo, Z. Chen, F.S. Wu, and Y.C. Chan, *J. Alloys Compd.* 673, 372 (2016).
7. Y. Li, F.S. Wu, and Y.C. Chan, *J. Mater. Sci: Mater. Electron.* 26, 8522 (2015).
8. Y.C. Chan and D. Yang, *Prog. Mater. Sci.* 55, 428 (2010).
9. C.-M. Chen, L.-T. Chen, and Y.-S. Lin, *J. Electron. Mater.* 36, 168 (2007).

10. X. Gu and Y.C. Chan, *J. Electron. Mater.* 37, 1721 (2008).
11. X. Gu, D. Yang, Y.C. Chan, and B.Y. Wu, *J. Mater. Res.* 23, 2591 (2008).
12. X.F. Zhang, H.Y. Liu, J.D. Guo, and J.K. Shang, *J. Mater. Sci. Technol.* 27, 1072 (2011).
13. C.-M. Chen and C.-C. Huang, *J. Alloys Compd.* 461, 235 (2008).
14. H. Sun, Y.C. Chan, and F. Wu, *J. Mater. Sci. Mater. Electron.* 26, 5129 (2015).
15. S. Ismathullakhan, H. Lau, and Y.-C. Chan, *Microsyst. Technol.* 19, 1069 (2012).
16. G. Xu, F. Guo, X. Wang, Z. Xia, Y. Lei, Y. Shi, and X. Li, *J. Alloys Compd.* 509, 878 (2011).
17. H. He, G. Xu, and F. Guo, *J. Mater. Sci.* 44, 2089 (2009).
18. T. Hu, Y. Li, Y.-C. Chan, and F. Wu, *Microelectron. Reliab.* 55, 1226 (2015).
19. D. Ma and P. Wu, *Mater. Sci. Eng. A* 651, 499 (2016).
20. M. Sona and K.N. Prabhu, *J. Mater. Sci. Mater. Electron.* 24, 3149 (2013).
21. S. Tian, F. Wang, X. Wang, and D. Li, *Mater. Lett.* 172, 153 (2016).
22. F. Wang, D. Li, S. Tian, Z. Zhang, J. Wang, and C. Yan, *Microelectron. Reliab.* 73, 106 (2017).
23. L.-T. Chen and C.-M. Chen, *J. Mater. Res.* 21, 962 (2006).
24. C. Chen and S.W. Liang, *J. Mater. Sci.* 18, 259 (2006).